Geochemical and Mineralogical Analysis of the Larsen Granodiorite, Miers Valley, Southern Victoria Land, Antarctica

Senior Thesis
Submitted in partial fulfillment of the requirements for the
Bachelor of Science Degree
At The Ohio State University

By

Kujtim L. Shaban
The Ohio State University
2015

Approved by

W. Berry Lyons, Advisor
School of Earth Sciences

Abstract

Miers Valley, Southern Victoria Land, Antarctica is located south of Marshall Valley and west of Koettlitz Glacier on the west coast of McMurdo Sound. It is part of the McMurdo Dry Valleys and is ice-free; the region is one of the world's most extreme deserts in the world. The basement rocks in the valley range from late Proterozoic to mid-Ordovician in age, with pre, post, and synkinemaic deformation occurring throughout. To provide a detailed view of the geochemical environment within Miers Valley, samples of the Larsen Granodiorite were examined for their geochemical, mineralogical and petrographic characteristics. X-ray Fluorescence (XRF) was used to obtain the bulk chemical composition of the Larsen Granodiorite. X-ray Diffraction (XRD) provided the mineralogical composition of this unit by randomly orienting the powdered sample to measure multiple d-spacing between crystal planes. Petrographic microscopy supplemented XRD analysis by providing mineralogical and textural descriptions of the samples. Data gathered via these methods were compared to previous regional studies and compared to upper continental crustal values. The analysis indicated the Larsen Granodiorite is relatively rich in intermediate rock elements of calcium, magnesium, manganese, and phosphorus compared to more felsic upper continental crustal values of silica and aluminum. Trace element data showed the Larsen Granodiorite is poor in nickel, copper, and sulfur, and rich in strontium, and niobium relative to upper continental crust. Mineralogy obtained through XRD indicated the Larsen Granodiorite is abundant in plagioclase and biotite contained within the andesine-labradorite series, and annite-phlogopite series, respectively, when compared to upper continental crustal values. Scanning electron microscopy (SEM) indicated trace amounts of the mineral allanite, (part of the broader epidote group) bearing rare earth elements of lanthanum, cerium, and neodymium. Petrographic analysis indicated partial straining of minerals and chloritized biotite possibly due to the migmatization of granitoid plutons.

Acknowledgements

This study is dedicated to Nancy Domi and Adrian Ginoli, with great affection.

First and foremost, I would like to thank Dr. W. Berry Lyons for his encouragement, patience, wisdom, and guidance with this research and critical comments that vastly improved this thesis. Thank you to The National Science Foundation (OPP 9118484) for funding the sample collection. A special thank you to Dr. Anne Grunow, Dr. John Encarnacion, and Byrd Polar Research Center Polar Rock Repository (NSF DPP 1141906) for collecting and providing the samples used in this study, for this thesis would not have been possible without their work in Miers Valley. Many thanks to Dr. Anne Carey and Dan Ardrey for facilitating the use of the X-ray Fluorescence and sample preparation. Thank you to Spectrum Petrographics Inc. for creating thin sections. A special thank you to Dr. Sue Welch for SEM, and X-ray Diffraction assistance and coordinating the procurement of thin section samples. Thank you to Ms. Kathy Welch and Mr. Chris Gardner of the Lyons Research Group for providing figures used in this study. Thank you to Dr. Julie Sheets and Michaela Wells for sample preparation and X-ray Diffraction assistance. A special thank you to Professor Sean O'Neill, the A-1 of mathematics.

Special thank you to Dr. Michael Barton and graduate fellow Christina Zerda for assistance with thin section analysis. Many thanks to my Sifu Lewis Charles for reinforcing the importance of open mindedness, focus and determination. Thank you, The Rolling Stones, who helped make time pass by seamlessly. Special thanks to my brother Ari Shaban for assisting with graphs, tables and putting up with my antics. Thank you to my mother Jeta Shaban, aunts and uncles, Lu Shurba, Vulka Domi, Nick Gani, Drita Scherer and dear friend Michael Rauh for support. Last but not least, thank you to my father Lou Shaban for encouragement and for making it possible to attend The Ohio State University, which ultimately led to this research being possible.

TABLE OF CONTENTS

List of Figures

List of Tables

Introduction

The McMurdo Dry Valleys region of Southern Victoria Land is the largest ice-free region on the continent of Antarctica (Levy 2013). Since the early 1960's the geology of the area has been studied by both United States and New Zealand geologists, in part, because of the extensive exposure of the bedrock, and it has direct access from the major US and New Zealand Antarctic Bases, i.e. McMurdo Station and Scott Base.

In fact, the bedrock geology of Southern Victoria Land has been broadly studied since the Heroic Age of Antarctic Exploration. However, the basement rocks of the area are inadequately investigated. This lack of knowledge is due to the fact that it is difficult to navigate the terrain, and the nature of the tectonic complexity contained within the Transantarctic Mountains (Stump, 1995).

Regional Geology

Miers Valley (MV) is one of the southern most parts of the McMurdo Dry Valleys region in Southern Victoria Land. MV is located between the Royal Society Range and west of Koettlitz Glacier, on the coast of South Victoria Land, slightly south of Marshall Valley and approximately 68 km SW from McMurdo Station (Figure 1, Appendix B). The valley is free of ice; and the bedrock within the valley is of late Precambrian to early Paleozoic in age. The rock types observed in MV are the Beacon Supergroup, and the Koettlitz Group containing the Larsen Granodiorite (Cox & Allibone, 1991).

The Beacon Supergroup consists of fine sandstone, shale, and coals of Permian age. The Beacon is intruded by the Jurassic Ferrar dolerite (Angino & Owen, 1962). The Koettlitz group and subsequently, the Miers Valley rock suite are metasediments, as originally described by Grindley & Warren (1964), and occur as greenschist-amphibolite facies, and amphibolite facies.

The Koettlitz Group contains primarily, marbles, schists, that are intercalate by gneisses and arkose, pre- and post-kinematic granitoid, gabbro and dike intrusions and the synkinematic Larsen Granodiorite.

The Koettlitz group of granitoids and metasediments form the basement rocks and are the oldest rocks in the Dry Valley system. The Larsen Granodiorite basement rocks as described by (Gunn & Warren, 1962) contain a westward dipping attitude, and are overlain by the Beacon Supergroup (Wright, 1980). Fold axes of plutonic margins trend NE-SW compression, with NW trending folds (Cox, 1989).

Three stages of deformation are observed in the Koettlitz Group and they include recumbent folds, upright tight folds, and upright folds, trending North-Northwest are projected around the southern shear zone of the Larsen Granodiorite suite (Findlay, et al., 1984). Smillie (1991) outlined several plutonic assemblages in the Taylor-Ferrar region according to their petrographic, geochemical characteristics and morphological features; aptly named Dry Valleys 1 and Dry Valleys 2, (DV1 and DV2) for short, the former being the oldest. The DV1 rock assemblage classified by (Smillie, 1989) are characterized by a metaluminous to peraluminous, calc-alkaline relationship. Plutons contained within the DV1 suite are generally granodiorites and granite-gneisses but also contain monzodiorites and granites. The DV1 suite contains the Bonney, Hedley, Valhalla, Catspaw, and Denton plutons. Pluton ages are late Precambrian to early Paleozoic in age, and age dating done by Deutsch & Groggler (1966), Faure & Jones (1974), via Sr/Rb, indicate that ages of formation occurred from late-Proterozoic through the mid-Ordovician. The DV2 rock assemblage are relatively rich in K_2O, Rb, and relatively poor in CaO, and V (Smillie, 1989). This latter group contains the Nibelungen, and Pearce Plutons. However, the rock types are similar to those from the DV1 suite, grading from monzodiorite to granite. (Cox & Allibone, 1991). In this study, the DV1 suite will be the primary focus since it serves as the host of the Miers Valley rock assemblage, explicitly the Larsen Granodiorite.

The Larsen Granodiorite suite is contained within the Hedley, Valhalla, Bonney and Denton plutons that form the DV1 suite. The Bonney pluton is the most understood pluton contained within the DV1 suite, due to its large distribution across the region (Cox & Allibone, 1991). Composing the Miers Valley southwest flank is an eastern trending belt of metamorphic rocks belonging to the Heald Member, which is overlain by the Chancellor Orthogneiss and contains rock types of the amphibolite facies, namely schists, and gneisses, which are relatively rich in biotite mica. The metasediments are intruded by the Larsen Granodiorite from the south and the west. Approaching Lake Miers to the North, the metasediments begin to trace the Larsen Granodiorite along its eastern boundary (Findlay et al., 1984) (Figure 2 Appendix B).

The nature of the formation of granitic-gneiss plutons and metasediments within the Koettlitz group has been disputed since the original studies conducted by Gunn & Warren (1962). The plutons are generally regarded as being pre-tectonic within the intrusive rock suite. Murphy (1971) describe the granitoids as originating from the Koettlitz Group through metamorphic processes. This argument was based in the appearances of potassium feldspar crystals which have augen-type shapes.

Augen-type features consist of relatively large (compared to the matrix) and lenticular grain sizes. These features are of shear-type deformation due to compressional stress, in which rocks have been subjected to metamorphism. Findlay (1982), divided granitoids into two rock suites consisting of melanocratic augen gneisses and leucocratic orthogneisses which contain the Chancellor and Salmon Valley Orthogneiss (Gunn & Warren, 1962; Mortimer, 1981). Even with these previous studies of Southern Victoria Land basement rocks, there is much work needed to describe the nature of and the origin of the granite-gneissic plutons.

Objectives

The purpose of this study was to provide a new look at the Larsen Granodiorite through detailed geochemical, and mineralogical descriptions of this unit from the western portion of the Miers Valley where no previous such analyses had been done. The first objective was to determine the mineral constituents and geochemical composition of the Larsen Granodiorite in Miers Valley. The second objective was to provide a petrographic description of the Larsen Granodiorite and to compare the petrographic data to the mineralogical information obtained via precise X-ray diffraction analysis. The final objective was to compare and contrast the geochemistry of these rock samples to upper continental crustal values and other granitoids in the Dry Valleys region in order to gain a better understanding of geological implications of similar rocks in Miers Valley.

Methods

Rock samples were collected in Miers Valley, south of Marshall Valley and west of Koettlitz Glacier, on the coast of Victoria Land, Antarctica (Figure 1). Samples were obtained by Dr. John Encarnacion and Dr. Anne Grunow, curator of the NSF supported Polar Rock Repository, The Ohio State University, in 1992 from a National Science Foundation grant. In this study the following analysis was conducted: geochemistry by X-ray Fluorescence (XRF), mineralogy by X-ray Diffraction (XRD), and petrography via a standard petrographic microscope. The geochemical analyses were accomplished using the PANalytical X-ray Fluorescence spectrometer, the mineralogy via a PANalytical X-ray Diffraction spectromenter with High Score Plus software, and a Leica DM750 P standard petrographic microscope was used for petrographic analysis. The mineralogy of the samples was also observed using a scanning electron microscope.

XRF

Glass beads for XRF analysis were prepared in the following manner: granodiorite samples were crushed into pieces with a muddler, then placed into a shatter box and powdered for one minute. 2.5015g of powdered granodiorite was weighed out and combined with 10.0083g of lithium tetraborate ($Li_2B_4O_7$). The powder was then mixed until thoroughly homogenized. The prepared sample was placed into a furnace to create a homogeneous glass bead for analyzing abundances of major compounds and trace elements. 2.5053g of rock powder and 10.0034g of lithium tetraborate ($Li_2B_4O_7$) were combined and the same process was used to create a glass bead for PRR-7367. These data were compared to the following USGS standard reference materials: QLO-1 (quartz-latite) and W-2 (diabase) and are shown in Tables 1 & 2 (Appendix A).

Petrography

Petrographic thin sections were prepared by Spectrum Petrographics Inc. 3315 NE 112th Ave Ste. B82 Vancouver, Washington. Thin sections of the Larsen Granodiorite were examined for mineral constituents, their relative abundance, structure for intrusive relationships, and flow differentiation. Petrographic analysis was conducted by observing prepared thin sections under plane light and cross-polarized light. Specific mineral content and relative abundances between samples were obtained using optical mineral characteristics in plane light such as cleavage planes, surface relief, and pleochroism. Cross-polarized light was used to determine such mineral features as extinction angles, twinning, optic axial planes, and birefringence.

Mineralogical proportions of both phenocrysts and matrix of the granodiorite samples were estimated using a mineral percent abundance estimation chart. This chart aids in the approximation of abundance of each mineral contained within the rock samples. Strategies included identifying the most abundant, darkest and opaque minerals first, as they are easiest to recognize in thin section. Second, the trace minerals were estimated, as they are easier to examine due to their relative low abundance within the samples. Finally, the accessory minerals were observed using the optical techniques noted above (Nesse, 2001). Characterization of feldspars in the MV samples was promoted via polarized light microscopy by examining characteristic twins synonymous with various feldspar compositions. Plagioclase was confirmed based on the properties of albite twinning. The Michael-Levy and Carlsbad-albite methods determined the plagioclase composition as the intermediate series andesine-labradorite. The potassium-rich feldspar microcline was confirmed based on characteristic crosshatch twins. Biotite is abundant, and a sizeable amount was oriented along its optical axis (the z-axis).

XRD

X-ray diffraction was conducted to identify specific mineral composition and thus crystallographic structure and orientation, which may be unobservable through petrographic analysis. Preparation of a powder was done in the following manner: a rock sample was placed into a shatter box for one minute and ground into a fine powder. The fine powder was then packed uniformly and tightly into an XRD sample disk. Bragg's Law ($n\lambda=2d\sin\theta$), (where n is an integer, λ is the wavelength of the x-ray and d is the distance between planes in the crystal lattice) (Nesse, 2001) was used to calculate the distance between atomic planes in each crystal lattice, and thus aided in the identification of minerals present within the MV sample sets. Since different minerals have a specific orientation within their respective crystal lattice, intensity values determined by XRD were divided by the angle 2θ, to provide the most accurate description of mineral constituents. Crystals were examined in several random orientations to determine the total number of d-spacings.

Results

Appendix A contains the bulk geochemistry of all major oxides, trace elements of the MV sample set, the USGS standards QLO-1 and W-2 for determining accuracy, precision measurements of the MV sample PRR-21025 and the USGS standard QLO-1 all of which are reported in Tables 1 & 2 (Appendix A). Dashed spaces indicate no data reported.

Silicon dioxide, aluminum oxide and calcium oxide are the most abundant constituents in the Larsen Granodiorite and range from 16.21-20.64%, 53.41-55.98% and 6.53-8.42%, and have a mean of 18.42%, 54.70%, and 7.46%, respectively. Manganese, titanium, and phosphorus oxides are among the least abundant major oxides, ranging from 0.05-0.16%, 0.83-1.22%, and 0.31-0.33%, and have a mean of 0.10%, 1.03%, and 0.32%, respectively.

The most abundant trace elements for PRR-7367 are strontium, barium, and zirconium, at 1,122, 789, and 194 ppm, respectively. The least abundant trace elements are nickel, germanium, and uranium at 0.420, 1.06, and 2.05 ppm, respectively.

The most abundant trace elements for PRR-21025 are barium, strontium, and vanadium at 915, 754, and 142 ppm. Germanium, uranium, and tantalum are among the least abundant trace elements for PRR-21025 at 1.08, 1.91, and 3.47 ppm.

The detection limits of all major compounds are presented in Table 3 (Appendix A). Dashes indicate lack of data due to the fact that the samples were below the detection limit of XRF analysis.

Appendix B comprises figures used in the study. Figure 1 shows the MV samples relative to samples from adjacent valleys within the McMurdo Dry Valley system. Figures 3 & 4 indicate the standard deviation of major compounds and trace elements of the MV sample set, respectively. XRD results of intensity vs 2θ for major minerals of MV samples PRR-7367 and PRR-21025 are presented in Figures 5 & 6, respectively. Figures 7 & 8 show intensity vs 2θ for secondary minerals of MV samples PRR-7367 and PRR-21025, respectively. Figures 9 & 10 show the similarity of chlorite and biotite for PRR-7367 and PRR-21025 respectively, where the d-spacings are in close proximity to one another, a possible indication of chloritization of biotite.

Figures 11 & 12 show the SEM elemental analysis indicating biotite of the annite-phlogopite series, and allanite, a rare earth element enriched mineral (part of the broader epidote group of sorosilicates).

Appendix C includes the petrographic thin section description of the Larsen Granodiorite samples PRR-7367 and PRR-21025 for which plagioclase and biotite are the major mineral constituents.

Discussion

Geochemistry

The Larsen Granodiorite major oxides and trace elements have been normalized to the upper continental crust values using data from Rudnick & Gao (2003). Figures 13 & 14 (Appendix B) indicate that the MV samples are low in titanium oxide and enriched in magnesium, calcium, and manganese oxide. The MV sample suite is poor in trace elements chromium, nickel, and cobalt and enriched in strontium, niobium, and tantalum.

Figure 15 (Appendix B) shows the relationship of strontium to rubidium concentrations. They are noticeably greater in the MV sample compared to the granites and granite-gneisses of Faure & Jones (1974) rock samples from Wright Valley, and upper continental crustal values of Rudnick & Gao (2003). Strontium can be a common trace element, especially in calcium-rich minerals as it can easily replace calcium as they both have similar size and charge (Faure, 1998). Figures 16 & 17 (Appendix B) display the MV major oxides and trace elements, relative to Rudnick & Gao (2003), showing the relationship among all sample sets. Figure 16 indicates that the MV sample PRR-7367 contains the lowest amount of manganese oxide relative to PRR-21025 and the upper continental crust. PRR-21025 is enriched in calcium, iron, and magnesium oxide relative to PRR-7367 and the upper continental crust.

The granodiorite samples analyzed from MV contain approximately 54.6% silica (SiO_2), which composes more than half of the total sample. This is consistent with previous work on the DV1 rock plutons of Headley and Valhalla biotite-granodiorites (Allibone et al., 1991). However, values from my samples differ by more than 10% in silica and 3% to 4% of calcium when compared to the composition of the upper continental crust, as reported by Rudnick & Gao (2003) (Figure 16, Appendix B). This is consistent with the fact that granodiorites are more mafic than the upper continental crust.

The MV samples contain less silica, and more iron, calcium, magnesium, manganese, and phosphorus oxides than average continental crust. On the other hand, aluminum, and potassium oxides in the MV rocks are relatively similar to continental crust concentrations given by Rudnick & Gao (2003) (Figure 16 Appendix B).

As noted above, the Larsen Granodiorite in Miers Valley is part of the DV1 granitoid suite and its geochemistry is consistent with the igneous type granitoids of the calc-alkaline variety as previously described by Smillie (1989). The standard deviation of the major oxides from the Miers Valley granodiorite suite relative to Rudnick and Gao (2003) average continental crust is 7.7%. The standard deviation of the individual MV samples is 7.9%. Phosphorus oxide and calcium oxide for PRR-7367 show the greatest percent enrichment of 118%, and 82%, respectively relative to upper continental crustal values. PRR-21025 shows a 112% and 134% percent enrichment of phosphorus and calcium oxide, respectively relative to upper continental crustal values.

The trace elements niobium, tantalum, and strontium show the largest percent enrichment for PRR-7367, relative to upper continental crustal values at 490%, 300%, and 250%, respectively. Similar to PRR-7367 albeit in different abundances, PRR-21025 trace elements tantalum, strontium, and niobium show the largest percent enrichments at 285%, 136%, and 115% relative to upper continental crustal values.

Relating PRR-7367 and PRR-21025 relative to upper continental crustal values indicate PRR-21025 is more abundant in transition metals chromium, cobalt, zinc, and nickel with percent diminished values of 107%, 88%, 69%, and 62%, respectively between the two samples. Sulfur, copper, nickel, and chromium are among the least abundant trace elements relative to upper continental crustal values with percent diminished values of 116%, 105%, 99%, and 97%, respectively.

A t-Test was conducted in order to determine if the means between the Larsen Granodiorite and upper continental crustal values were significantly different (Table 4, Appendix A). Since t-Stat is less than t-Critical, the null hypothesis is not rejected, as there was no observable variance between the sampled means. That is to say, the null hypothesis was neither accepted nor rejected based on the small sample size of the Larsen Granodiorite and still may contain a variance when compared to Rudnick & Gao (2003), (Figures 13 & 14, Appendix B).

Measurements of the concentrations of calcium oxide, and iron oxide vary considerably, up to 9.5% by weight compared to upper continental crust values. Rudnick & Gao (2003) report calcium and iron oxide concentrations of 3.6%, and 5.0%, respectively.

Compared to Rudnick & Gao (2003) upper continental crustal values, the Larsen Granodiorite shows higher concentrations of calcium, titanium, and phosphorus oxides (Figure 16 Appendix B). This is expected in more intermediate rocks, such as granodiorites, since they contain larger abundances of sodium and calcium due to plagioclase, a primary mineral constituent by definition. The concentration of trace elements in the Larsen Granodiorite normalized to Rudnick & Gao (2003) is shown in Figure 14 (Appendix B).

Mineralogy

Petrographic analysis indicates that the Larsen Granodiorite samples, PRR-21025 and PRR-7367 both contain plagioclase and biotite in relative high abundances, compared to the other mineral constituents. Secondary minerals consist of quartz, amphibole, pyroxene; trace amounts of zircon, and apatite are also present. Refer to Appendix C for a complete petrographic description of the MV suite.

XRD is useful for determining mineral constituents in rocks samples that are difficult to view or are nearly indistinguishable with a standard petrographic microscope. In general, the mineral assemblage determined by petrographic analysis is confirmed by the mineralogy determined via XRD.

XRD indicated that the main variety of plagioclase observed in thin section is of the andesine-labradorite series and biotite is found to be an intermediate composition of the annite-phlogopite series (Figure 5, Appendix B). The chloritization of biotite observed in thin section is consistent with XRD analysis, as shown in Figures 9 & 10 (Appendix B).

The close d-spacings suggest an overlap in chlorite and biotite. XRD results reveal that both PRR-7367and PRR-21025 are intermediate to calcic-rich (Figures 5 & 6, Appendix B). In general, both samples are mineralogically analogous, albeit some variations within the range of members between the minerals. PRR-7367 is more abundant than PRR-21025 in the intermediate to calcic rich plagioclase member labradorite. PRR-21025 is shown to contain more of the pyroxene diopside than augite than does PRR-7367. The dominant variety of plagioclase contained within PRR-21025 ranges from andesine-labradorite (Figure 6, Appendix B), an intermediate series of plagioclase with an anorthite percentage ranging from 30% to 70% (An_{30-70}). It contains cleavage planes in three different directions with intersections approaching 90°. Plagioclase in PRR-21025 grades into areas containing the oligoclase variety, an intermediate member of plagioclase, with an anorthite percentage ranging from 10% to 30% (An_{10-30}). However, largely plagioclase rich, PRR-21025 also grades into areas containing the potassium rich feldspar microcline, which was confirmed by petrographic microscopy by its characteristic crosshatch twinning.

XRD analysis indicates PRR-7367 contains more labradorite than PRR-21025. The large abundance of biotite in PRR-21025 is shown to contain the annite-phlogopite series. Annite is the iron rich end-member and phlogopite, the magnesium rich end-member. The biotite composition in PRR-21025 lies in-between this series as determined by SEM analysis (Figure 11, Appendix B), and PRR-7367 contains a similar compositional variety of biotite to PRR-21025. Biotite is extensively chloritized throughout both samples of the Larsen Granodiorite, possibly due to the migmatization of granitoid plutons. In some instances, biotite has been completely altered to chlorite, as observed in thin section, and confirmed through XRD analysis as shown in Figures 9 and 10 (Appendix B). Secondary minerals of the sample sets include quartz, chlorite, amphiboles such as hornblende and pyroxenes such as augite and diopside (Figures 7 and 8, Appendix B). SEM analysis of PRR-21025 shows the sample contains allanite, a rare earth element enriched mineral (Figure 12, Appendix B).

Conclusions

Major conclusions of this study:

- Aluminum, silicon, and calcium oxides are the most abundant oxides present. Manganese, titanium, and phosphorus are among the least abundant oxides in the Larsen Granodiorite.

- The Larsen Granodiorite, which is part of the basement lithology in Miers Valley, is an intermediate rock suite, rich in calcium magnesium, manganese, and phosphorus relative to upper continental crustal values. Aluminum, and potassium are relatively similar when compared to the upper continental crust.

- PRR-21025 has more iron, calcium, and magnesium oxide. Whereas, PRR-7367 is slightly more alkali-rich, this is most likely due to variations in the mineral phases of plagioclase and a larger presence of potassium feldspar.

- Trace elements strontium, niobium, and tantalum are relatively high, and sulfur, copper, chromium, and nickel are relatively low compared to continental crust.

- PRR-21025 is more abundant in more abundant in transition metals of chromium, cobalt, zinc, and nickel relative to PRR-7367.

- The Larsen Granodiorite is more abundant in calcium and contains the amphibole hornblende, and clinopyroxenes augite, and diopside whereas the granodioritic gneisses of the Dry Valleys region observed by Cox & Allibone (1991) often lack the appearance of amphibole and clinopyroxene.

- Overall, the Larsen Granodiorite shows a similar pattern of major oxides to those of upper continental crustal values.

Recommendations for Future Research

As I have only analyzed two samples of the Larsen Granodiorite form Miers Valley, recommendations for future work include analysis of other samples from the McMurdo region in order to describe any variability of this lithology. Future research could address the petrographic and structural concerns, and speculate on the origin of and relationships between basement granitoids in the Dry Valleys system and the processes that shaped and deformed the region, as formulated by earlier investigations of this lithology.

References Cited

Allibone, A.H., Forsyth, P.J., Turner, I.M., Sewell, R.J., and Bradshaw, M.A. (1991) Geology of the Thudergut Sheet, southern Victoria Land, Anatarctica. 1:500000 N.Z.G.S. Map and notes; Wellington, New Zealand: Department of Scientific and Industrial Research.

Angino, E.E., and Owen, D.E. (1962) Sedimentologic Study of Two Members of the Beacon Formation, Windy Gully, Victoria, Land, Antarctica. *Trans. Kansas Acad. Sci.* 65(1), 61-69.

Angino, E.E., Turner, M, and Zeller, E.J. (1962) Reconnaissance geology of lower Taylor Valley, Victoria Land, Antarctica. *Bulletin of the Geological Society of America* ***73,*** 1553-1562.

Cox, S.C. (1989) Gneiss geology- A structural perspective of foliated granitoids and their host rocks in the Wright Valley, South Victoria Land, Antarctica. M.Sc. thesis, University of Otago, New Zealand, 185 [Unpublished].

Cox, Simon C., and Allibone, Andrew H. (1991) Petrogenesis of Orthogneiss in the Dry Valleys region, South Victoria Land. Antarctic Science **3**, 405-407, 415-416.

Deutsch, S. and Groggler, N. (1966) Isotopic age of the Olympus-granite gneiss (Victoria Land, Antarctica). *Earth and Planetary Science Letters,* **1**, 82-84.

Faure, G. (1998) Principles and Applications of Geochemistry (2nd ed.). Upper Saddle River, NJ: Prentice-Hall, Inc.

Faure, G. and Jones, L.M. (1974) Isotopic composition of strontium and geologic history of the basement rocks of Wright Valley, southern Victoria Land, Antarctica. *New Zealand Journal of Geology and Geophysics,* ***17****, 611-627.*

Findlay, R.H. (1982) Basement geology of the McMurdo Sound region, Antarctica. Report to the Ross Dependency Research Commission, 50 [Held in the Antarctic Division D.S.L.R. Library, Chrishchurch, New Zealand [Unpublished].

Findlay, R.H., Skinner, D.N.B. and Craw, D. (1984) Lithostratigraphy and structure of the Koettlitz Group McMurdo Sound, Antarctica. *New Zealand Journal of Geology and Geophysics*, **27**, 513-536.

Grindley, G.W., Warren, G. (1984) Stratigraphic nomenclature and correlation in the western part of Ross Sea. in: Adie, R.J. ed. *Antarctic Geology.* Amsterdam, North Holland Publishing Co., 314-333.

Gunn, B.M. and Warren, G. (1962) Geology of Victoria Land between the Mawson and Mulock Glaciers, Antarctica. *New Zealand Geological Survey Bulletin*, **71**, 157.

Levy, J. (2013) How big are the McMurdo Dry Valleys? Estimating ice-free area using Landsat image data. *Antarctic Science*, **25**, 119-120.

Mortimer, G. (1981) Provisional report on the geology of the basement complex between Miers and Salmon valleys. *New Zealand Antarctic Record,* ***3****, 1-8.*

Murphy, D.J. (1971) The petrology and deformational history of the basement complex, Wright Valley, Antarctica, with special reference to the origin of augen gneisses. Ph.D thesis, University of Wyoming, U.S.A., 114 [Unpublished].

Nesse, W. (2001) *Introduction to Mineralogy*. (2nd ed.). Oxford, UK: Oxford University Press (OUP).

Rudnick, R.L., and Gao, S. (2003) Composition of the Continental Crust. Treatise on Geochemistry, **3**, 4-6, 18.

Smillie, R.W. (1989) Granite Harbour Intrusives, Taylor and Ferrar Glacier region, southern Victoria Land, Antarctica. M.Sc. thesis, University of Otago, New Zealand, 247 [Unpublished].

Smillie, R.W. (1991) In press. Suite subdivision and petrological evolution of granitoids from the Taylor Valley and Ferrar Glacier region, south Victoria Land. *Antarctic Science*.

Stump, E. (1995) The Ross Orogen of the Transantarctic Mountains. Cambridge University Press, New York.

Wright, A.C. (1980) A reconnaissance study of the McMurdo Volcanics northwest of the Koettlitz Glacier. *Antarctic record* **I(2)**, 10-15.

Appendix A

Compilations of Geochemical Data

And Statistical Analysis

Major Compounds						
Seq.	Sample name (1-12)	Al_2O_3	SiO_2	Fe_2O_3	CaO	TiO_2
1 [1]	W-2	15	51	11	10	1.1
2 [1]	W-2	15	51	11	10	1.1
3 [1]	W-2	15	51	11	10	1.1
4 [1]	QLO-1	16	62	4.2	3.0	0.58
5 [1]	QLO-1	16	62	4.2	3.0	0.58
6 [1]	QLO-1	16	62	4.2	3.0	0.59
7 [2]	PRR-7367	21	56	5.0	6.5	0.83
8 [2]	PRR-7367	21	56	5.0	6.5	0.83
9 [2]	PRR-7367	21	56	5.0	6.5	0.83
10 [2]	PRR-21025	16	54	9.5	8.5	1.2
11 [2]	PRR-21025	16	53	9.5	8.4	1.2
12 [2]	PRR-21025	16	53	9.5	8.4	1.2
	[3] Calculated Precision	±0.12	±0.04	±0.21	±0.24	±1.64
	[4] Calculated Precision	±0.19	±0.47	±0.13	±0.08	±0.03

Table 1. Compilation of major compounds obtained by XRF analysis.
[1]Standard Samples
[2]Miers Valley Samples
[3]Calculated Precision PRR-21025
[4]Calculated Precision QLO-1 (standard)

Major Compounds (Continued)						
Seq.	Sample name (1-12)	MgO	MnO	K_2O	Na_2O	P_2O_5
1 [1]	W-2	6.4	0.17	0.60	2.2	0.13
2 [1]	W-2	6.4	0.17	0.59	2.2	0.13
3 [1]	W-2	6.4	0.17	0.60	2.2	0.13
4 [1]	QLO-1	0.96	0.090	3.4	4.2	0.26
5 [1]	QLO-1	0.96	0.090	3.4	4.1	0.26
6 [1]	QLO-1	0.96	0.090	3.4	4.2	0.26
7 [2]	PRR-7367	2.3	0.050	2.2	4.9	0.33
8 [2]	PRR-7367	2.3	0.050	2.2	4.9	0.33
9 [2]	PRR-7367	2.3	0.050	2.2	4.9	0.33
10 [2]	PRR-21025	6.4	0.16	2.8	3.0	0.32
11 [2]	PRR-21025	6.4	0.16	2.8	3.0	0.32
12 [2]	PRR-21025	6.4	0.16	2.8	3.0	0.32
	[3] Calculated Precision	±0.31	±13	±0.71	±0.66	±6.3
	[4] Calculated Precision	±0.07	-	±0.12	±0.13	±0.020

Table 1. Compilation of major compounds obtained by XRF analysis.
[1]Standard Samples
[2]Miers Valley Samples
[3]Calculated Precision PRR-21025
[4]Calculated Precision QLO-1 (standard)

Trace Elements							
Seq.	Sample name (1-12)	Ba	Co	Cr	Cu	Ni	S
1 [1]	W-2	170	43	73	98	65	210
2 [1]	W-2	170	42	72	97	66	210
3 [1]	W-2	180	42	73	97	65	190
4 [1]	QLO-1	1300	8.1	2.6	25	2.1	2.0
5 [1]	QLO-1	1200	6.7	1.7	25	1.7	1.7
6 [1]	QLO-1	1300	7.4	1.4	24	2.9	1.7
7 [2]	PRR-7367	780	14	2.3	-	-	-
8 [2]	PRR-7367	790	13	3.6	-	0.90	-
9 [2]	PRR-7367	790	13	3.7	-	0.43	-
10 [2]	PRR-21025	920	28	100	7.9	29	-
11 [2]	PRR-21025	910	28	100	7.6	29	-
12 [2]	PRR-21025	920	29	100	8.0	29	-
	[3] Calculated Precision	±0.0020	±0.070	±0.020	±0.26	±0.070	±0.030
	[4] Calculated Precision	±80	±0.50	±1.7	±3.0	-	-

Table 2. Compilation of trace elements obtained by XRF analysis in parts per million (ppm).
[1]Standard Samples
[2]Miers Valley Samples
[3]Calculated Precision PRR-21025
[4]Calculated Precision QLO-1 (standard)

Trace Elements (Continued)							
Seq.	Sample name (1-12)	Sr	V	Zn	Zr	Th	Y
1 [1]	W-2	190	270	74	67	2.0	17
2 [1]	W-2	190	270	74	67	2.0	17
3 [1]	W-2	190	260	74	66	2.0	16
4 [1]	QLO-1	300	59	53	130	5.7	22
5 [1]	QLO-1	300	59	53	130	5.7	22
6 [1]	QLO-1	300	57	53	130	5.7	23
7 [2]	PRR-7367	1100	88	65	190	7.3	21
8 [2]	PRR-7367	1100	85	66	190	7.3	22
9 [2]	PRR-7367	1100	86	66	190	7.3	20
10 [2]	PRR-21025	760	140	100	88	5.9	22
11 [2]	PRR-21025	750	140	100	88	5.9	22
12 [2]	PRR-21025	750	140	100	89	5.9	22
	[3] Calculated Precision	±0.0030	±0.010	±0.020	±0.023	±0.34	±0.090
	[4] Calculated Precision	±12	±6.0	±3.0	±16	±0.50	±3.0

Table 2. Compilation of trace elements obtained by XRF analysis in parts per million (ppm).

[1]Standard Samples

[2]Miers Valley Samples

[3]Calculated Precision PRR-21025

[4]Calculated Precision QLO-1 (standard)

Trace Elements (Continued)				
Seq.	Sample name (1-12)	Nb	Ta	U
1 [1]	W-2	2.0	0.24	1.3
2 [1]	W-2	2.1	0.28	1.3
3 [1]	W-2	2.1	0.25	1.3
4 [1]	QLO-1	26	2.3	1.8
5 [1]	QLO-1	26	2.3	1.8
6 [1]	QLO-1	26	2.3	1.8
7 [2]	PRR-7367	70	3.6	2.0
8 [2]	PRR-7367	71	3.6	2.0
9 [2]	PRR-7367	71	3.6	2.0
10 [2]	PRR-21025	26	3.5	1.9
11 [2]	PRR-21025	26	3.5	1.9
12 [2]	PRR-21025	26	3.5	1.9
	[3] Calculated Precision	±0.080	±0.58	±1.1
	[4] Calculated Precision	±1.3	±0.10	±0.12

Table 2. Compilation of trace elements obtained by XRF analysis in parts per million (ppm).
[1]Standard Samples
[2]Miers Valley Samples
[3]Calculated Precision PRR-21025
[4]Calculated Precision QLO-1 (standard)

[1] Lower Limit of Detection (ppm)									
Al_2O_3	SiO_2	Fe_2O_3	CaO	TiO_2	MgO	MnO	K_2O	Na_2O	P_2O_5
120	-	7.0	27	9.3	30	3.4	9.7	4.4	7.0
120	-	7.0	26	9.3	31	3.4	9.6	4.4	7.1
120	-	7.0	27	9.4	31	3.4	9.6	1.8	7.1
130	-	5.9	24	8.7	31	3.1	8.5	5.5	7.2
130	-	5.9	24	8.7	30	3.1	8.5	6.0	7.3
130	-	5.9	24	8.6	31	3.1	8.5	6.4	7.2
120	-	5.5	19	8.1	27	3.0	10	-	6.5
120	-	5.5	18	8.0	28	3.0	10	-	6.7
120	-	5.5	19	8.1	28	3.0	10	-	6.5
120	-	7.1	28	9.0	29	3.3	4.8	-	4.7
120	-	7.1	28	9.0	29	3.3	4.7	-	4.6
120	-	7.1	28	8.9	29	3.3	4.8	-	4.4

Table 3. Compilation of the lower limit of detection obtained by XRF analysis.
[1]Lower limit of detection is the smallest amount of an element in the sample set that can be detected by the XRF.

t-Test					
Output	PRR-7367	Rudnick & Gao	Output	PRR-21025	Rudnick & Gao
Mean	9.88	9.50	Mean	10.15	9.50
Variance	298.51	423.07	Variance	256.32	423.07
Observations	10.00	10.00	Observations	10.00	10.00
Pearson Correlation	0.99	-	Pearson Correlation	0.98	-
Hypothesized Mean Difference	0.50	-	Hypothesized Mean Difference	0.50	-
df	9.00	-	df	9.00	-
t Stat	-0.09	-	t Stat	0.08	-
P(T<=t) one-tail	0.47	-	P(T<=t) one-tail	0.47	-
t Critical one-tail	1.83	-	t Critical one-tail	1.83	-
P(T<=t) two-tail	0.93	-	P(T<=t) two-tail	0.94	-
t Critical two-tail	2.26	-	t Critical two-tail	2.26	-

Table 4. t-Test to determine if the sample means were significantly different.

Appendix B

Figures

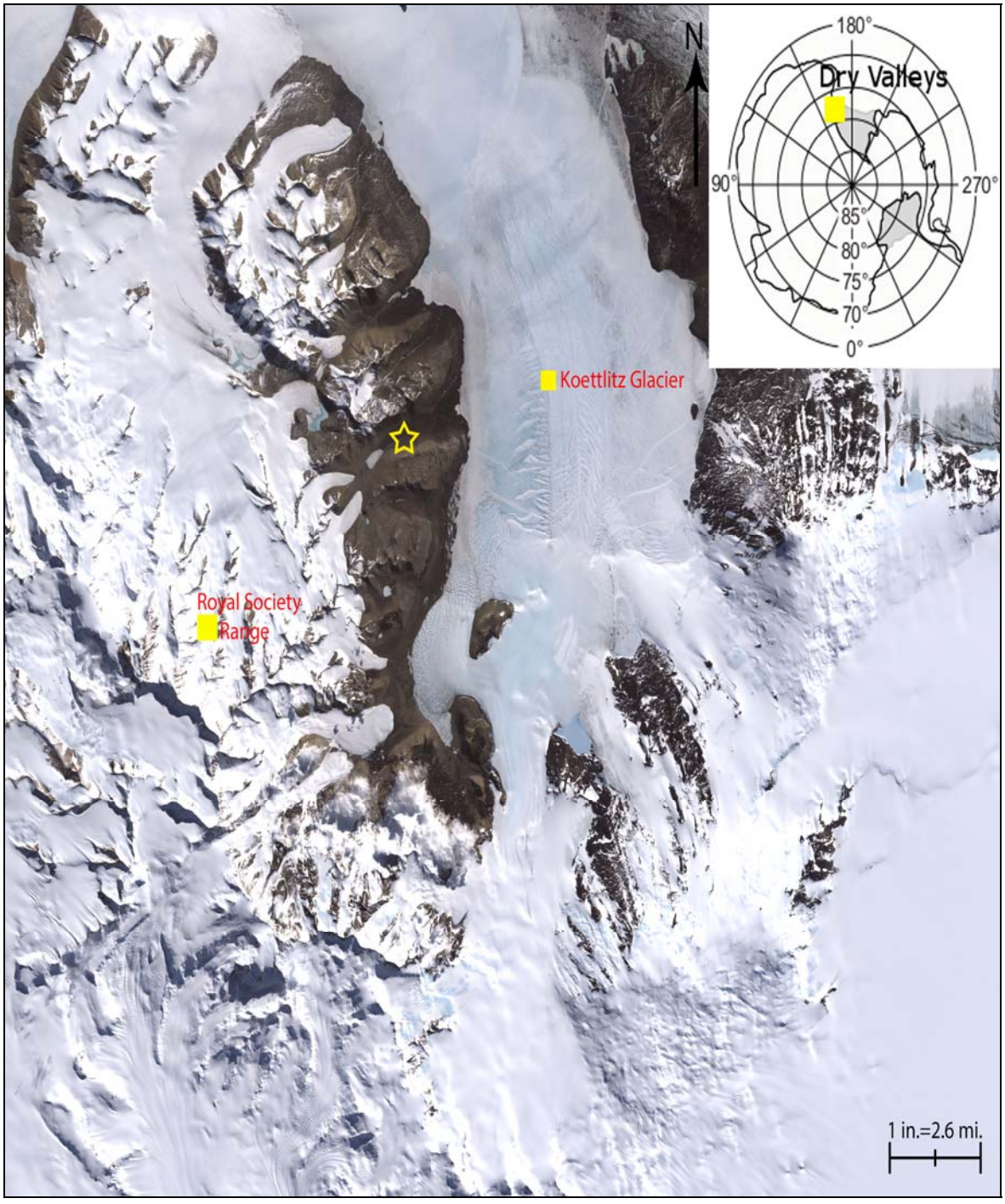

Figure 1. Regional map of the southern Dry Valleys. Location of MV samples denoted by the star. The adjacent Koettlitz Glacier and Royal Society Range shown for reference.

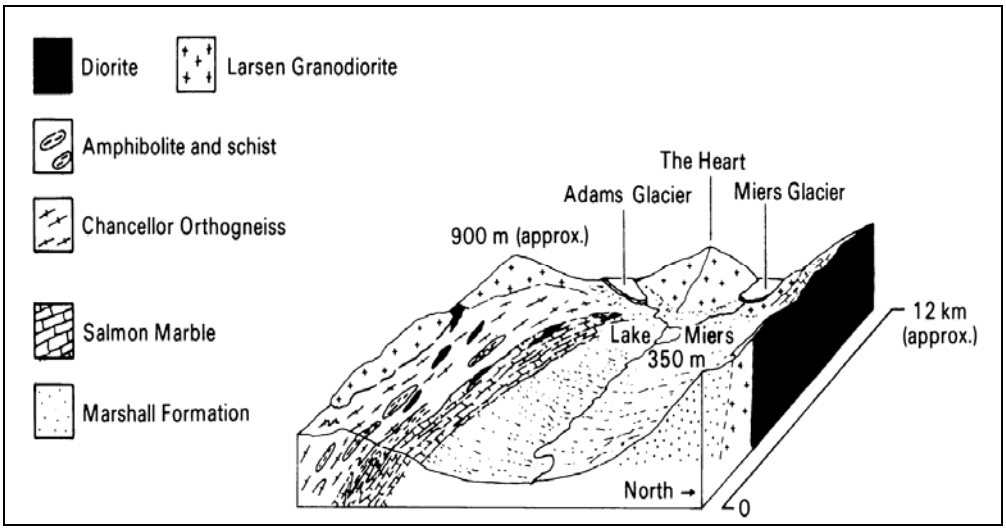

Figure 2. Block Diagram indicating the distribution of the lithological units and their location within Miers Valley (Figure 14 from Findlay et al. 1984).

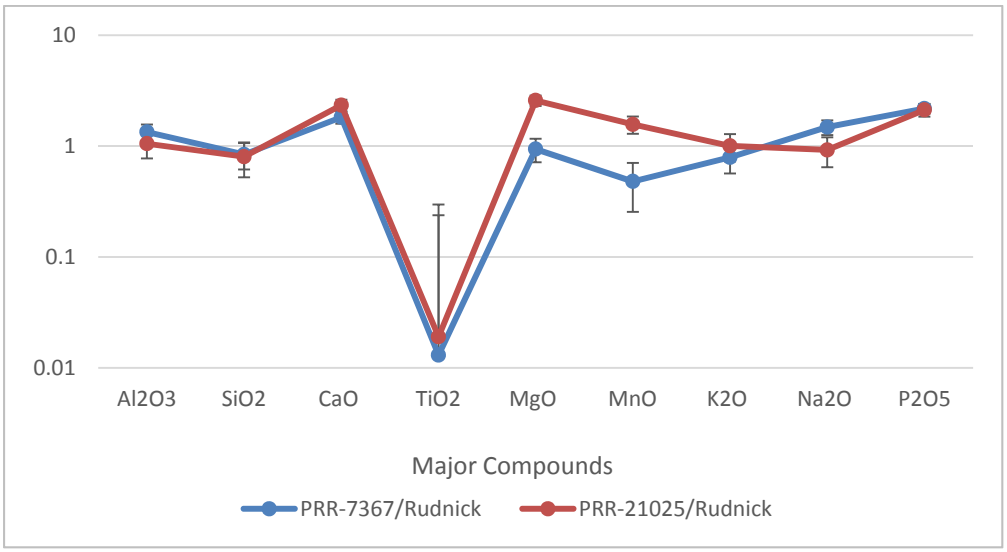

Figure 3. Standard deviation between MV major compounds normalized to oxide concentrations of Rudnick and Gao (2003).

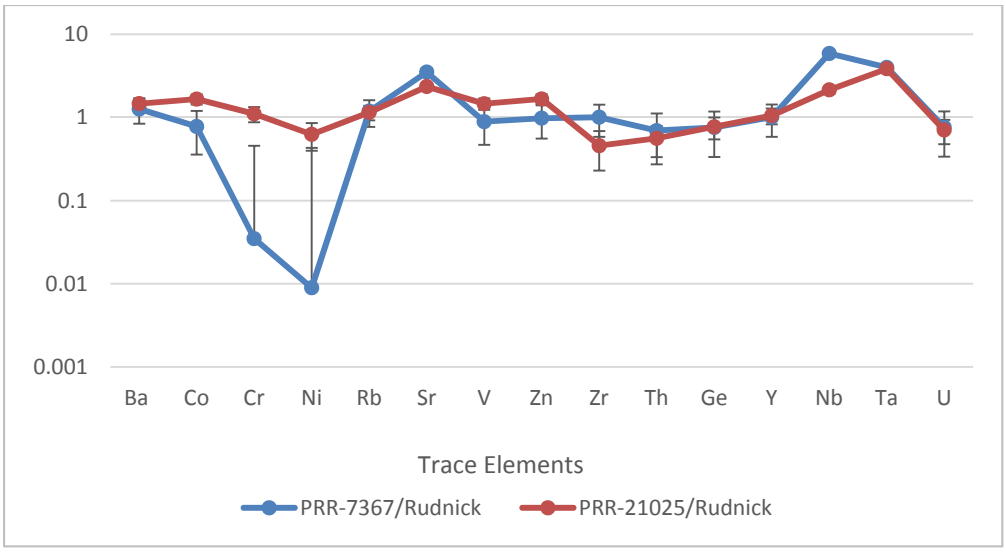

Figure 4. Standard deviation between MV trace elements normalized to Rudnick and Gao (2003).

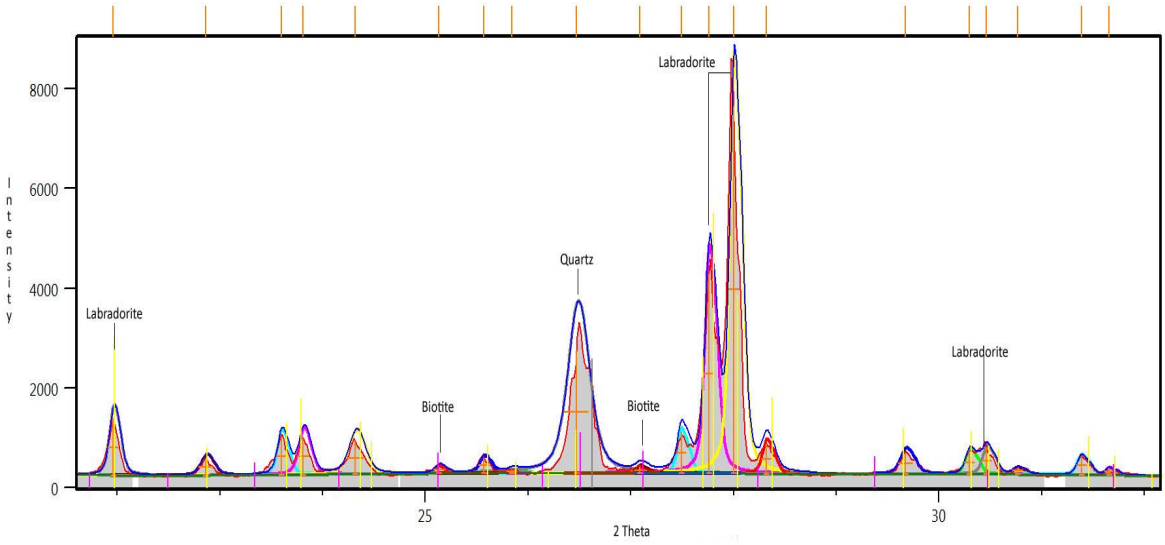

Figure 5. Intensity versus 2 Theta, indicating major minerals based on their d-spacings as determined by XRD for sample PRR-7367.

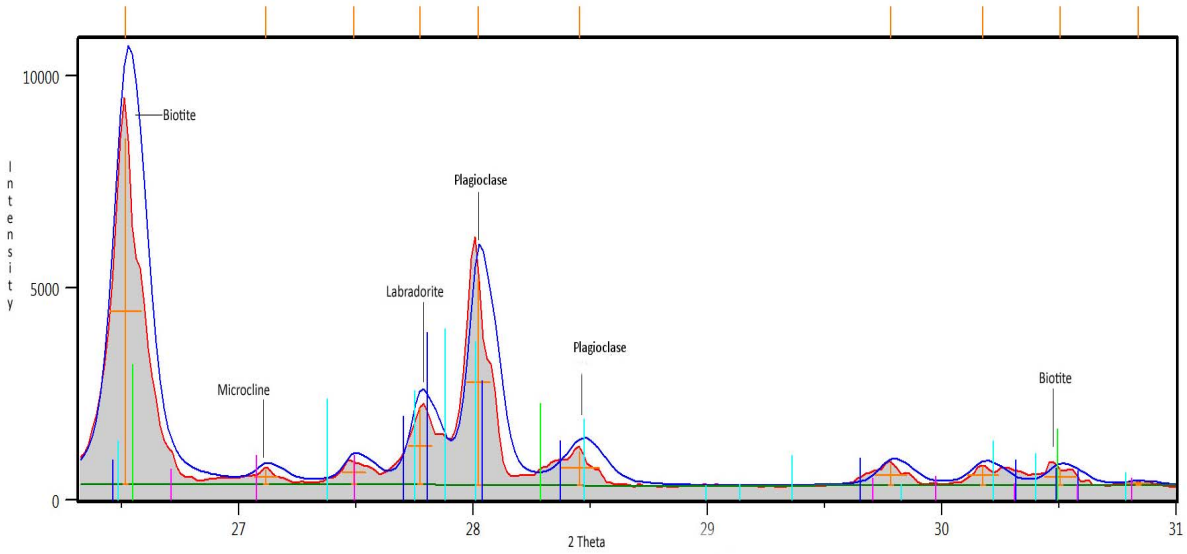

Figure 6. Intensity versus 2 Theta, indicating major minerals based on their d-spacings as determined by XRD for sample PRR-21025.

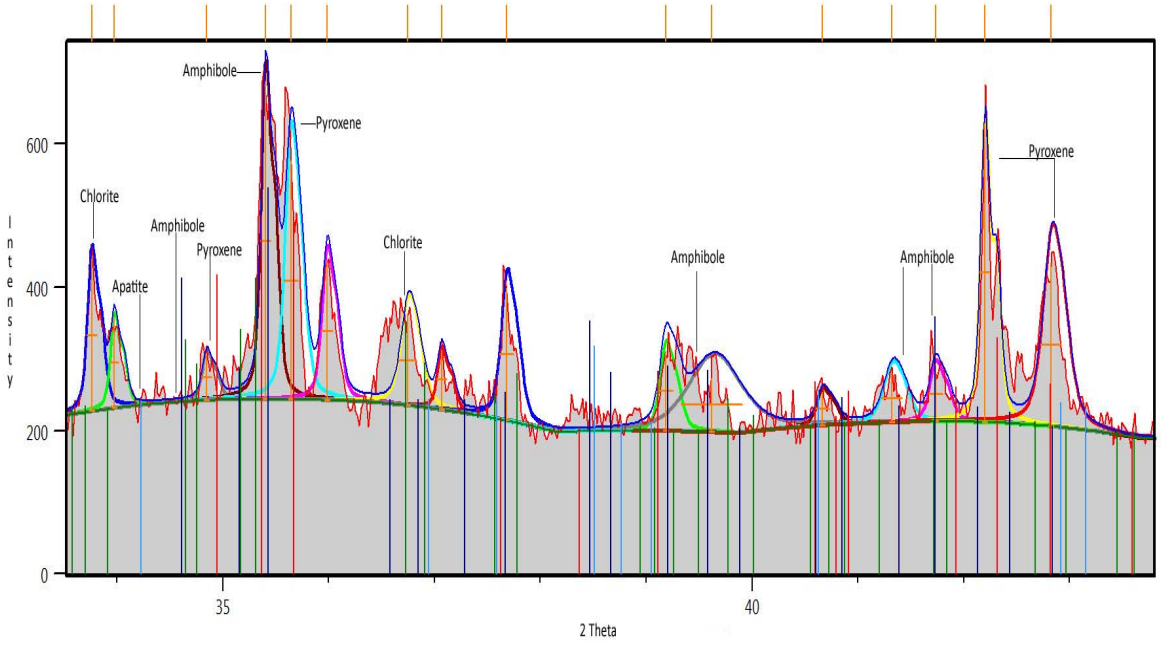

Figure 7. Intensity versus 2 Theta, indicating secondary minerals based on their d-spacings as determined by XRD for sample PRR-7367.

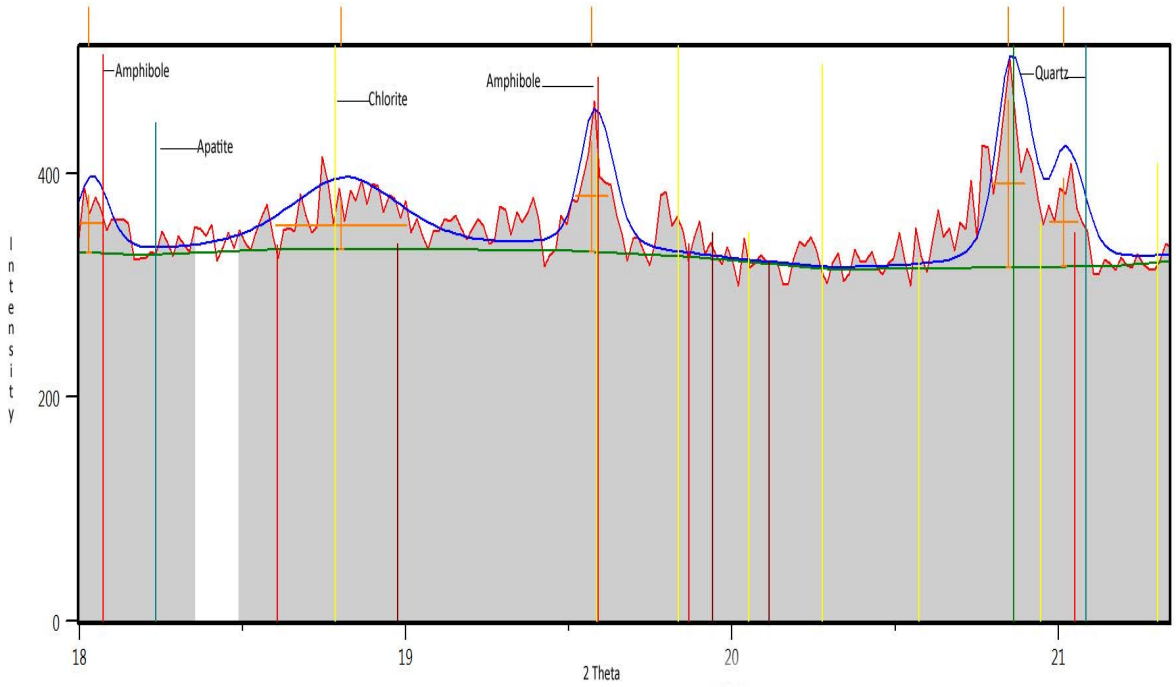

Figure 8. Intensity versus 2 Theta, indicating secondary minerals based on their d-spacings as determined by XRD for sample PRR-21025.

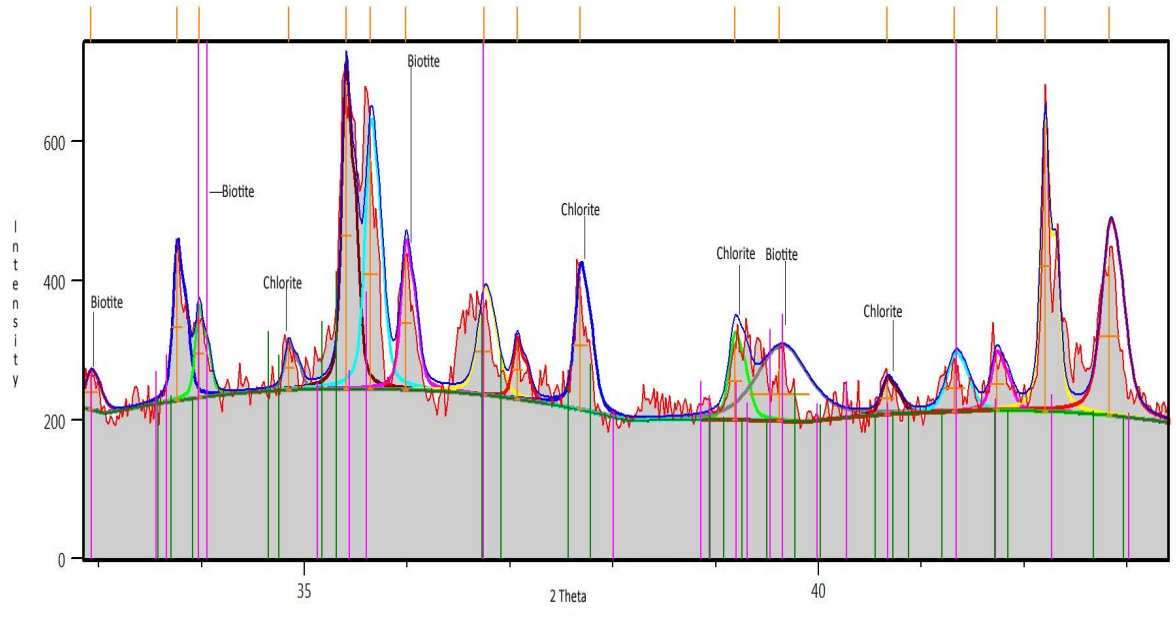

Figure 9. Intensity versus 2 Theta, indicating biotite and chlorite based on their d-spacings as determined by XRD for sample PRR-7367.

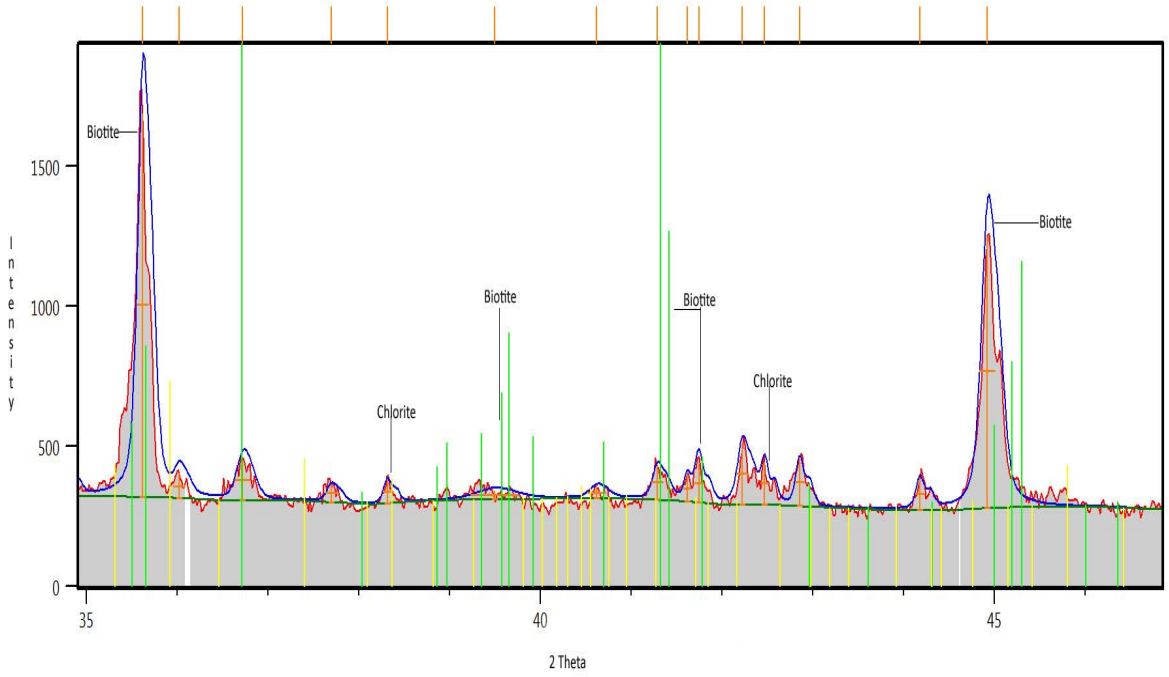

Figure 10. Intensity versus 2 Theta, indicating biotite and chlorite based on their d-spacings as determined by XRD for sample PRR-7367.

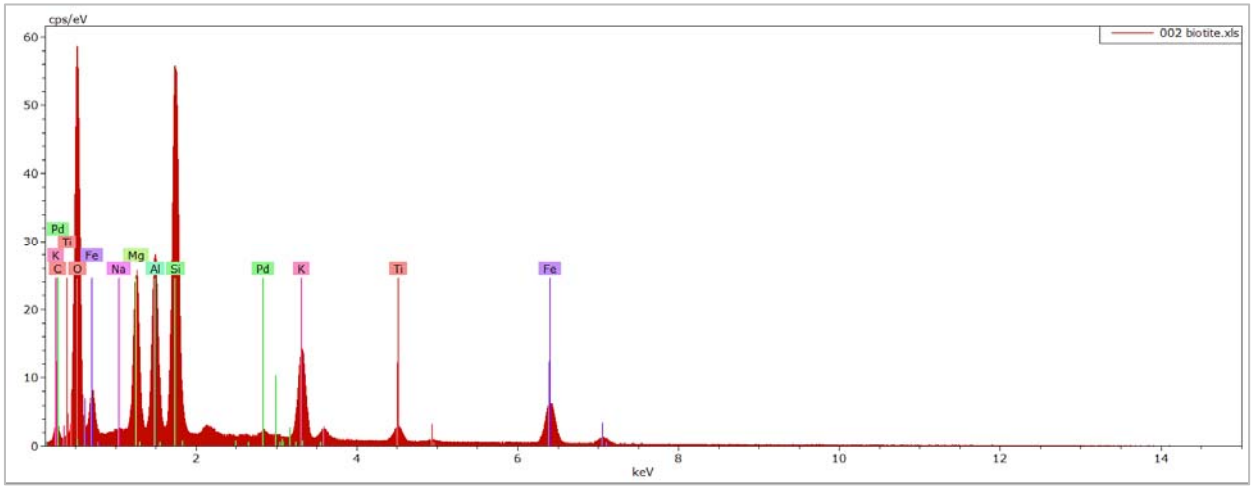

Figure 11. SEM elemental data indicating the mineral biotite. An intermediate form of biotite between the annite-phlogopite series, as indicated by the intensities of iron and magnesium.

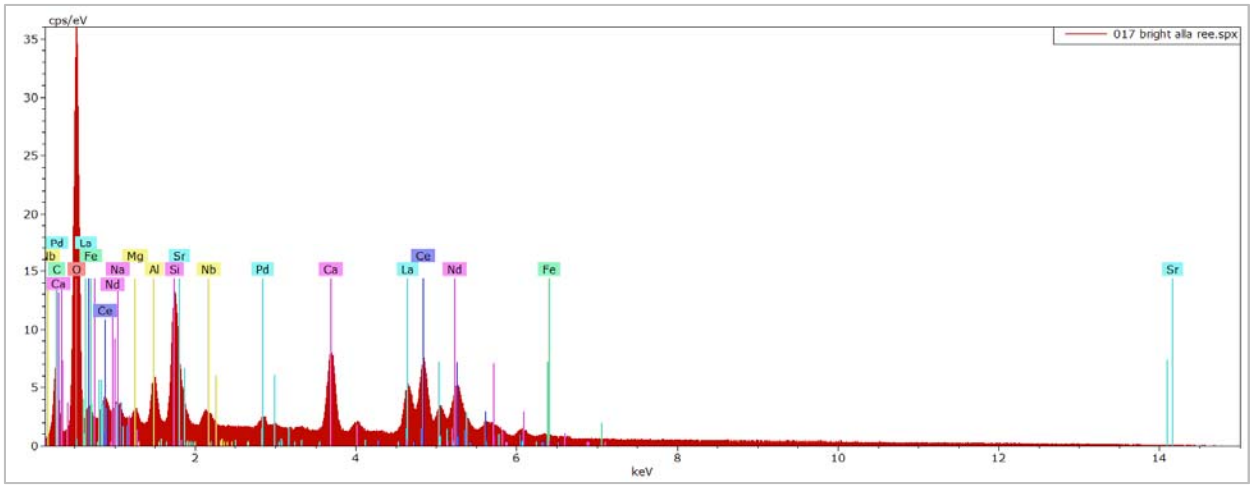

Figure 12. SEM elemental data indicating the mineral allanite, containing the rare earth elements of lanthanum, cerium, and neodymium.

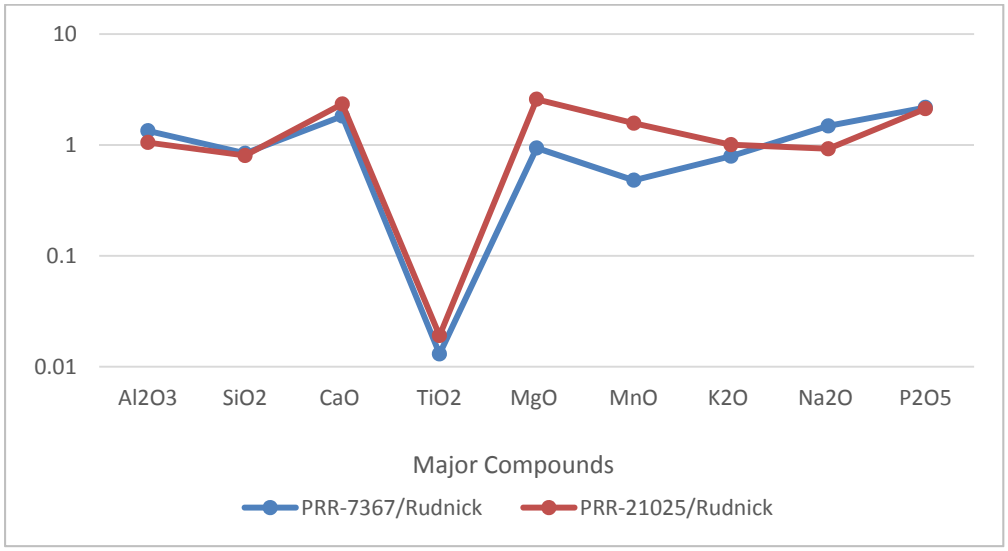

Figure 13. Miers Valley granodiorite major oxides normalized to upper continental crustal values of Rudnick & Gao (2003).

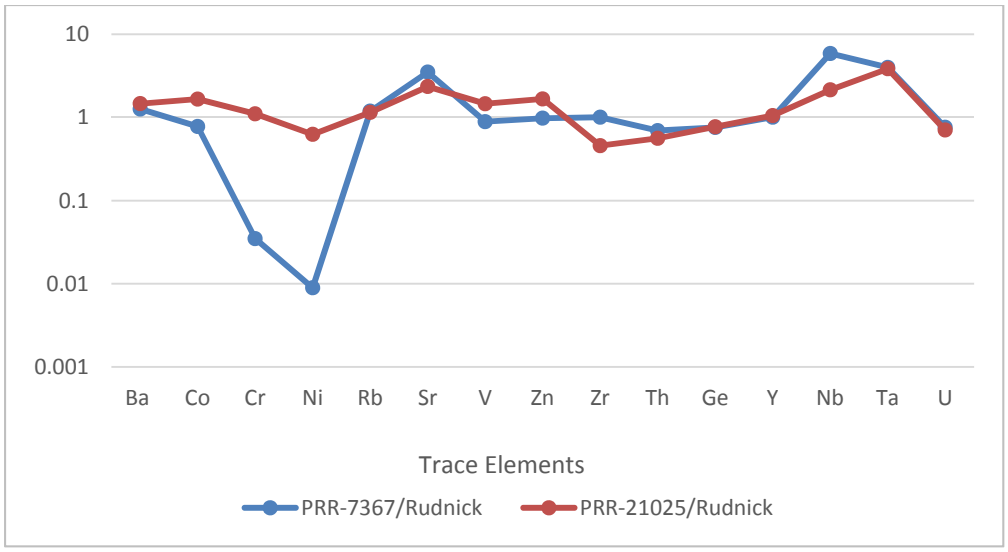

Figure 14. Miers Valley granodiorite trace elements normalized to upper continental crustal values of Rudnick & Gao (2003).

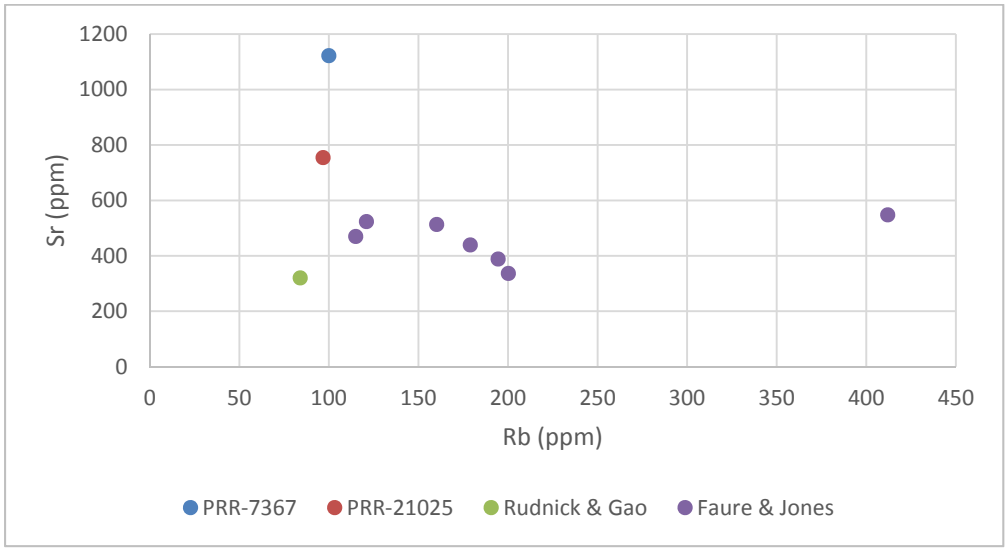

Figure 15. Strontium versus rubidium of the Miers Valley granodiorite compared to Sr/Rb of the upper continental crust from Rudnick and Gao (2003) and granite-gneisses from Faure & Jones (1974) in Wright Valley, Southern Victoria Land, Antarctica.

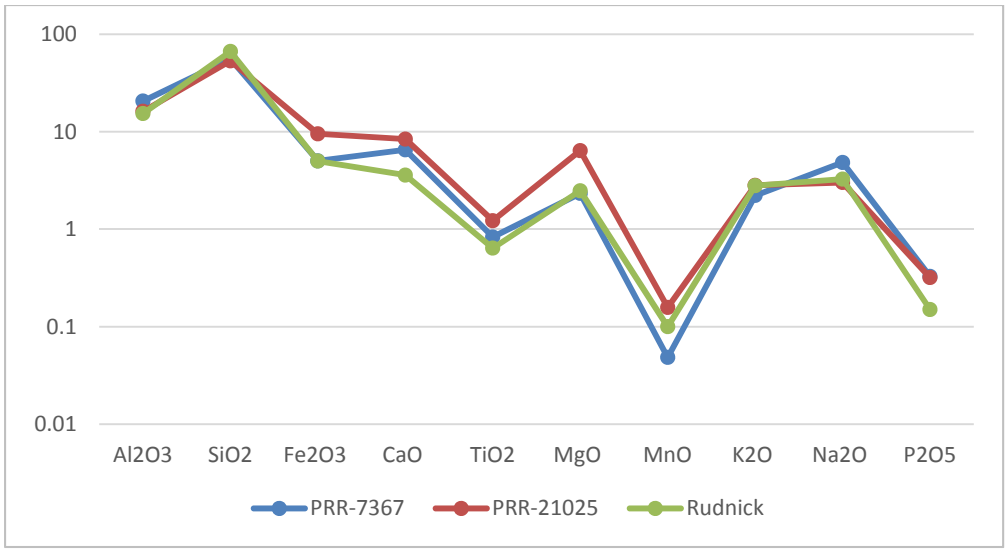

Figure 16. Major oxides of Miers Valley granodiorite relative to upper continental crustal values of Rudnick & Gao (2003).

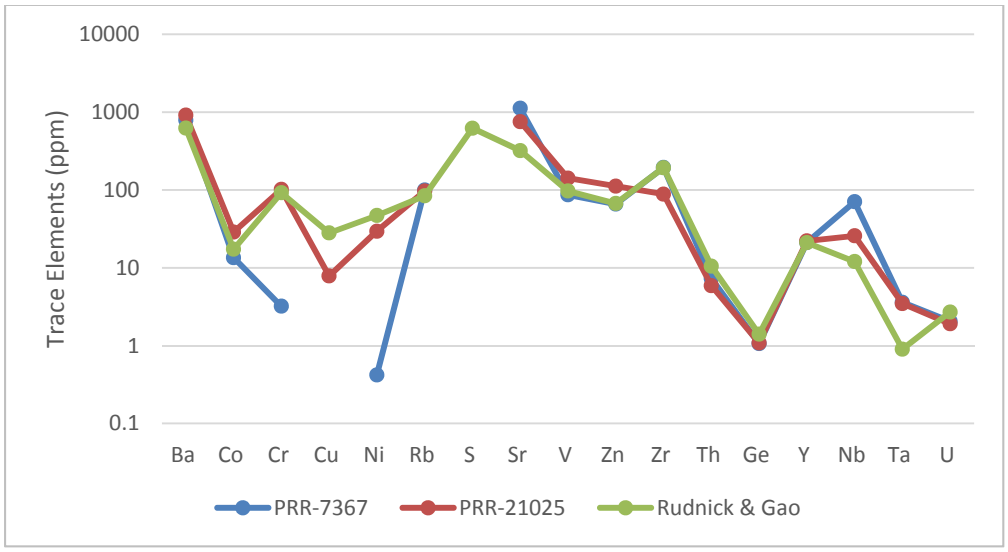

Figure 17. Trace elements of Miers Valley relative to Rudnick & Gao (2003).

Appendix C

Thin Section Description

Thin Section Description

PRR-7367 Biotite Granodiorite

Granodiorite: A medium grained (1-5mm), hypidiomorphic rock, with phenocrysts of plagioclase, biotite, and opaques in a matrix of mostly plagioclase, some alkali feldspar in the form of microcline, and disseminated opaques. Biotite mica and plagioclase are abundant. Quartz present albeit, relatively lower in abundance than plagioclase or biotite. Chloritized biotite present, probably chloritization through alteration due to pre and post-kinematic stresses. This sample grades into areas containing microcline, observed by its characteristic crosshatch twinning. Due to the relatively low abundance of quartz and the abundance of alkali feldspar to plagioclase feldspar in the matrix and the relative large abundance of biotite, suggests this rock is a biotite granodiorite. Approximate modal percentage of minerals in thin section: 60%

Phenocrysts

Plagioclase. Crystal sizes up to 3.5mm in length, subhedral, many contained in aggregates of intergrown crystals. Some grains contain inclusions of biotite, chlorite, apatite, and opaque minerals. Some crystals are poikilitically enclose opaque grains. Hypidiomorphic textures are observed. Plagioclase composition determined as part of the andesine series, but this sample grades into areas containing the oligoclase variety. Polysynthetic albite twinning is most common; twinning on the Carslbad-albite laws observed. The angle of the rhombic structure varies from ±2-3 degrees and albite twinning is widespread on the {010} crystal face.

Biotite. Subhedral crystals of 0.5-1.0mm in length, are abundant within the sample; contains dark halos possibly due to radioactive inclusions. Brown to brown-green in color. Different axes orientations present on the X axis color is projected as yellow. On the Y=Z axis down the center of the crystal lattice, color is projected as dark brown. Biotite is partially strained and chloritized.

Quartz. Subhedral crystals ranging 0.5-1.0mm in length. Relatively low in abundance in matrix, especially compared to that of plagioclase and biotite.

Hornblende. Though hornblende is typically lacking in abundance, large subhedral to euhedral phenocrysts occur, ranging 0.3-1.5mm in length contained within plagioclase. Sample contains inclusions of subhedral quartz. Often shown in the X-axis plane, shown to be colorless.

Secondary Minerals

Chlorite. Crystals ranging 0.1-0.3mm in length. As noted above, chlorite occurs mostly as chloritized biotite. However, complete alteration from biotite to chlorite was observed.

Clinopyroxene. Crystal sizes range 0.5-1mm in length. Pyroxene in the form of augite, and diopside.

Microcline. Crystal sizes up to 1mm in length 66% anorthite 34% albite; potassium feldspar (microcline) occurs interstitially.

Accessory Minerals

Apatite. Crystal sizes 0.025-0.075mm in length. Euhedral inclusions of apatite occur within plagioclase, biotite, hornblende, forms prismatic crystals with hexagonal cross sections.

Sphene. Crystal sizes 0.025-0.075mm in length. High relief, and dark brown –brown in thin section. Pleochroism: very weak

Zircon. Euhedral crystals of zircon, sizes up to 0.5mm. Zircon occurs as chadacrysts within plagioclase.

Opaque Minerals

Possible magnetite, ilmenite, of crystal lengths of 0.025-0.075mm

Matrix

The groundmass consists of plagioclase laths, biotite, and quartz. Secondary minerals of clinopyroxene, amphibole, and chlorite with minor opaques. Plagioclase composition is mainly of the andesine variety. Ferromagnesian minerals of the amphibole group and pyroxenes represented with moderate to high interference colors.

Mineral Proportions

Phenocrysts	*40%*
Plagioclase	*20%*
Biotite	*15%*
Quartz	*3.0%*
Hornblende	*2.0%*
Matrix	*60%*

PRR-21025 Quartz-Biotite Granodiorite

Granodiorite: A medium grained (1-5mm), hypidiomorphic rock, that grades into areas of panidiomorphic texture. Encompasses phenocrysts of plagioclase, biotite, quartz, and chlorite within a matrix of mostly plagioclase, and biotite with opaques. Chadacrysts of biotite and quartz within the oikocrysts of plagioclase. Partially strained plagioclase and biotite probably due to pre, post, and synkinematic tectonic stresses. Fluid inclusions are contained within sample. Biotite present throughout sample in a relative large abundance to that of other constituent minerals. Partially chloritized biotite easily observed, with instances of chlorite itself from the complete alteration of biotite. The low abundance of quartz relative to plagioclase implies this is a granodiorite. Approximate modal percentage of minerals in thin section: 55%.

Phenocrysts

Plagioclase. Crystals up to 3.5mm in length. Hypidiomorphic observed to be of the andesine-labradorite series; grades into areas containg the oligoclase variety. Plagioclase is mostly contained within the matrix, albeit phenocrysts are invariably present. Polysynthetic albite twinning most common, however the sample contains Carlsbad twins, zoning, and cross-hatch twinning. Albite twinning present on {010} facies. Fluid inclusions present.

Biotite. Crystal size 1.0-2.5mm in length. Biotite oriented along x and z axes. The x axis shows the mineral to be yellow in color, along the y=z axis the color is shown to be dark brown.

Quartz. Crystals of 0.5-1.0mm in length. Subhedral grains. Fluid inclusion present within plagioclase, and hornblende 0.5-1mm.

Hornblende. Subhedral phenocrysts occur, ranging 0.3-1.5mm in length contained within plagioclase.

Secondary Minerals

Clinopyroxene. Crystal sizes range 0.5-1.5mm in length. Pyroxene in the form of diopside.

Chlorite. Crystals of 0.5-1.5mm in length. Present as partially chloritized biotite as well as instances of pure chlorite assumed to be produced by alteration from biotite.

Accessory Minerals

Apatite. Crystal sizes 0.025-0.075mm in length. Euhedral inclusions of apatite occur within plagioclase, biotite, hornblende, forms prismatic crystals with hexagonal cross sections.

Sphene. Crystal sizes 0.025-0.075mm in length. High relief, and brown to brown in thin section. Pleochroism: very weak.

Zircon. Euhedral crystals of zircon, sizes up to 0.5mm. Zircon occurs as chadacrysts within plagioclase.

Opaque Minerals

Possible magnetite, ilmenite of crystal lengths of 0.025-0.075mm.

Matrix

The groundmass consists of plagioclase laths, biotite, and quartz respectively in abundance. Secondary minerals of augite, hornblende, and chlorite with minor opaque minerals. Plagioclase composition is mostly of the Labradorite variety grades into areas of Bytownite. Ferromagnesian minerals of the amphibole group and pyroxenes represented with moderate to high interference colors.

Mineral Proportions

Phenocrysts	*45%*
Plagioclase	*22%*
Biotite	*12%*
Quartz	*8.0%*
Hornblende	*3.0%*
Matrix	*55%*